

Merjenje energije

- osnove kalorimetrije

a) zakaj kalorimetri?

b) EM plaz \rightarrow EM kalorimeter

c) ločljivost EM kalorimetrov

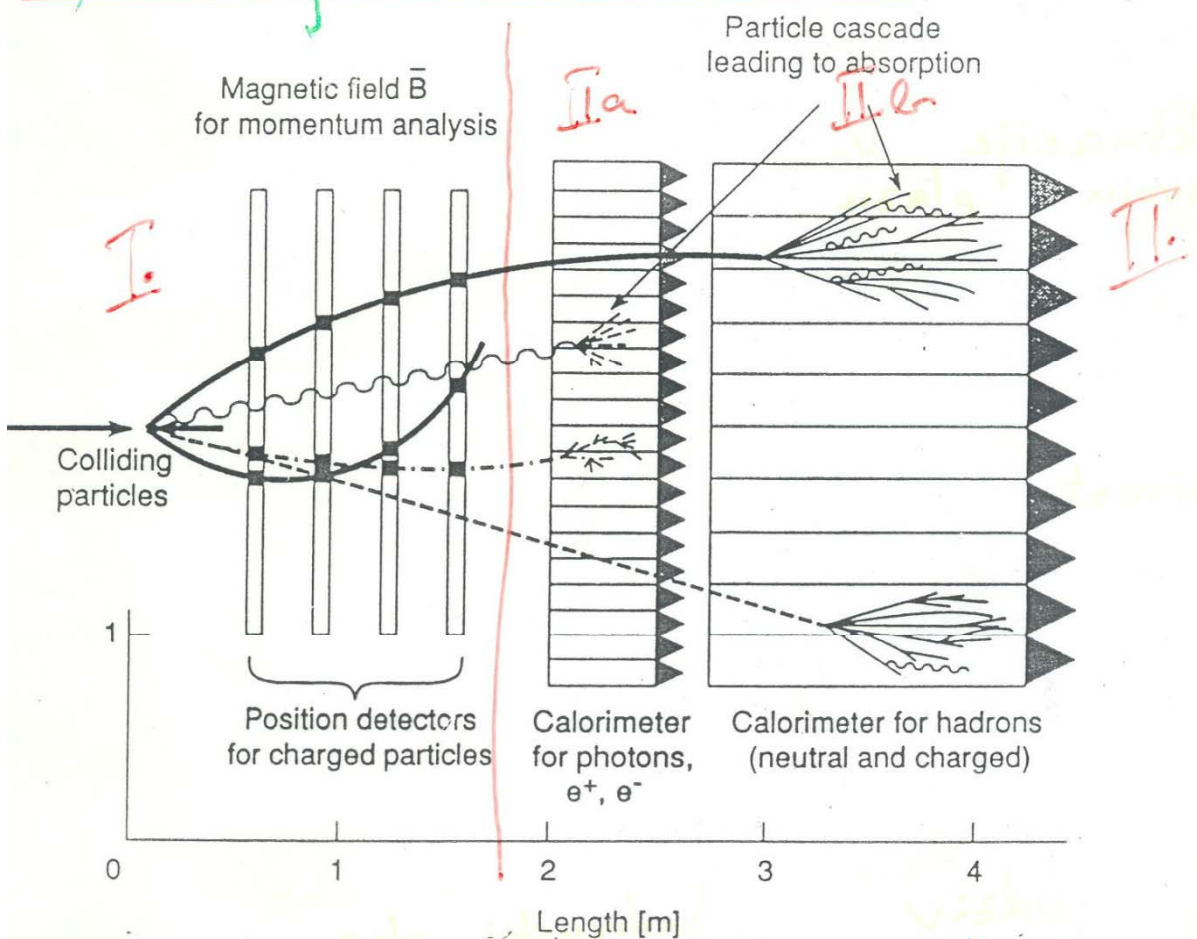
d) vzorcevanje

e) hadronski plaz \rightarrow hadronski kalorimeter

f) ločljivost hadronskih kalorimetrov

g) identifikacija s. kalorimetri

a) zakaj kalorimetri?



eksperiment \rightarrow meritev $p^\mu = (E, \vec{p})$

\vec{p}, E ali \vec{p}, m ali \vec{p}, v

I - $p = e B r$ sledilni sistem

II - meritev E s popolno absorbcojo in zaznavo odložene energije

Kalorimeter II.a EM e, γ

II.b hadronski π, K, p, n

odziv kalorimetra

- energija } delca
- vrsta } delca

absorbacija (npr. število sek. delcev - N)
 statistični proces $\rightarrow \frac{G_E}{E} \propto \frac{1}{\sqrt{E}}$

pouprečni odziv ponovljivost - ložljivost

prednosti kalorimetra za visoke E

$$-\frac{G_E}{E} \propto \frac{1}{\sqrt{N}} = \frac{1}{\sqrt{N}} \propto \frac{1}{\sqrt{E}}$$

ložljivost se izboljšuje! se slabša!

$$- L \propto \ln E$$

velikost narašča počasneje!

$$- e, \gamma, \pi^+, \pi^0, K^+, K^0, p, n$$

itnem. vse delce

$$- pljusk: E_{jet}$$

preprosta rekonstrukcija pljuskov
 \Rightarrow proženje

- hermetičnost

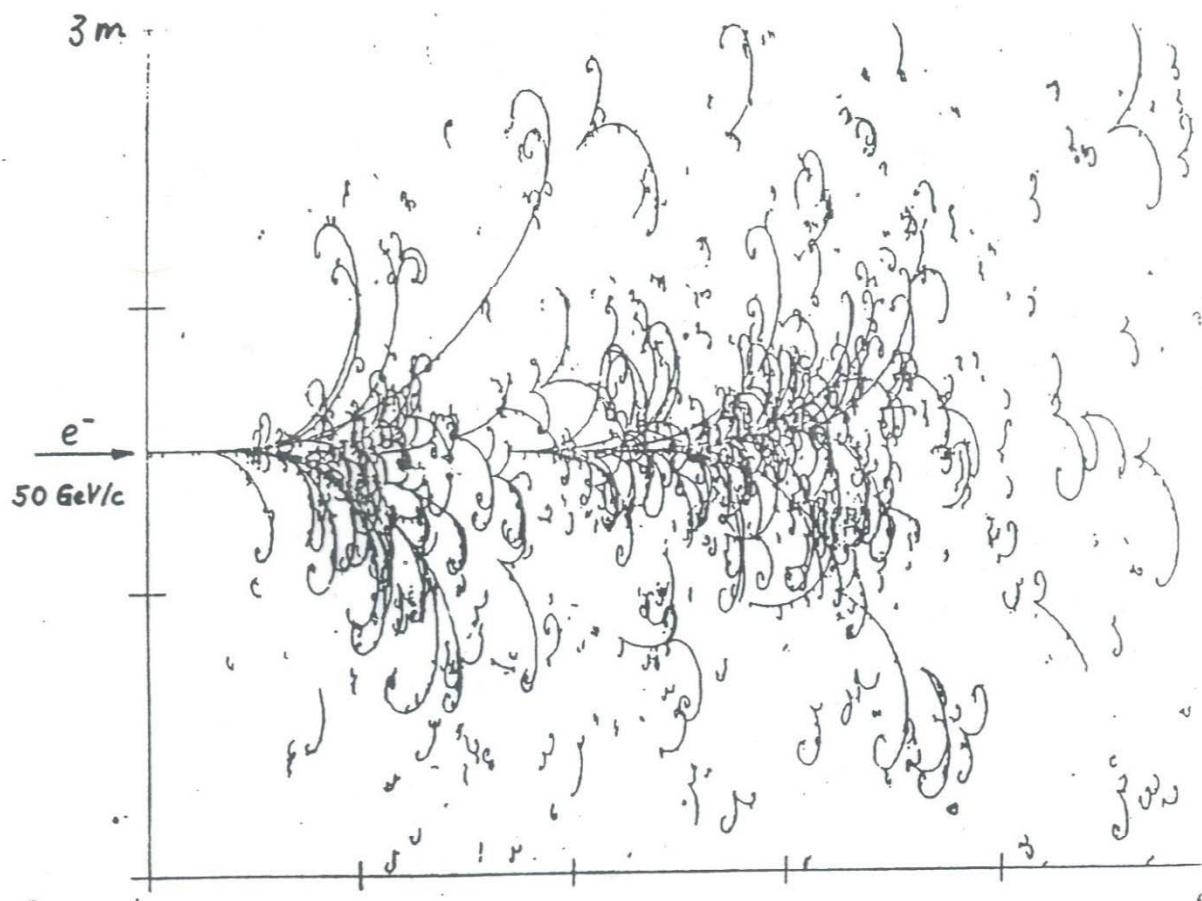
celoten dogodek \Rightarrow neutrini, SUSY

III EM plaz

3

e^- ali γ z visoko energijo $E_0 \gg E_c$

pari \rightarrow zavorno sevanje \rightarrow pari $\rightarrow \dots$



B EBC , Ne/H₂ (70/30%) , $\beta = 3T$

ELECTROMAGNETIC SHOWER DEVELO.

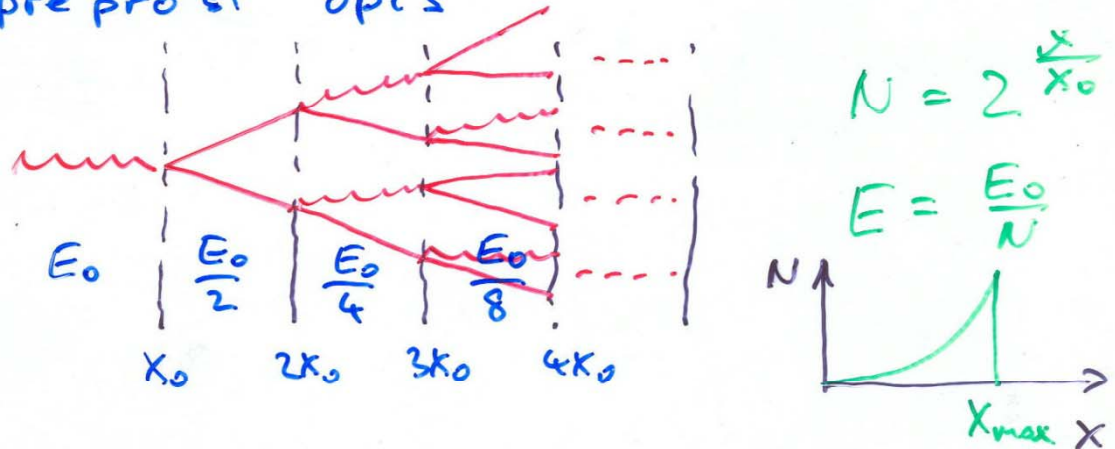
plaz raste dokler e^{\pm} izgubljajo

33

več energije = zavornim sevanjem
kot z ionizacijo - E_c

statični proces

pre prost opis



maksimalna dolžina $E = E_c$

$$x_{\max} = \frac{\ln \frac{E_0}{E_c}}{\ln 2} \quad (44)$$

$$N_{\max} = \frac{E_0}{E_c} \quad (45)$$

dolžina (velikost detektorja) narašča
kot $\ln E_0 \rightarrow$ kalorimetri

poznamo posamične procese \Rightarrow

MC simulacija EM plazu
EGS (\rightarrow v GEANT)

longitudinalna oblika

34

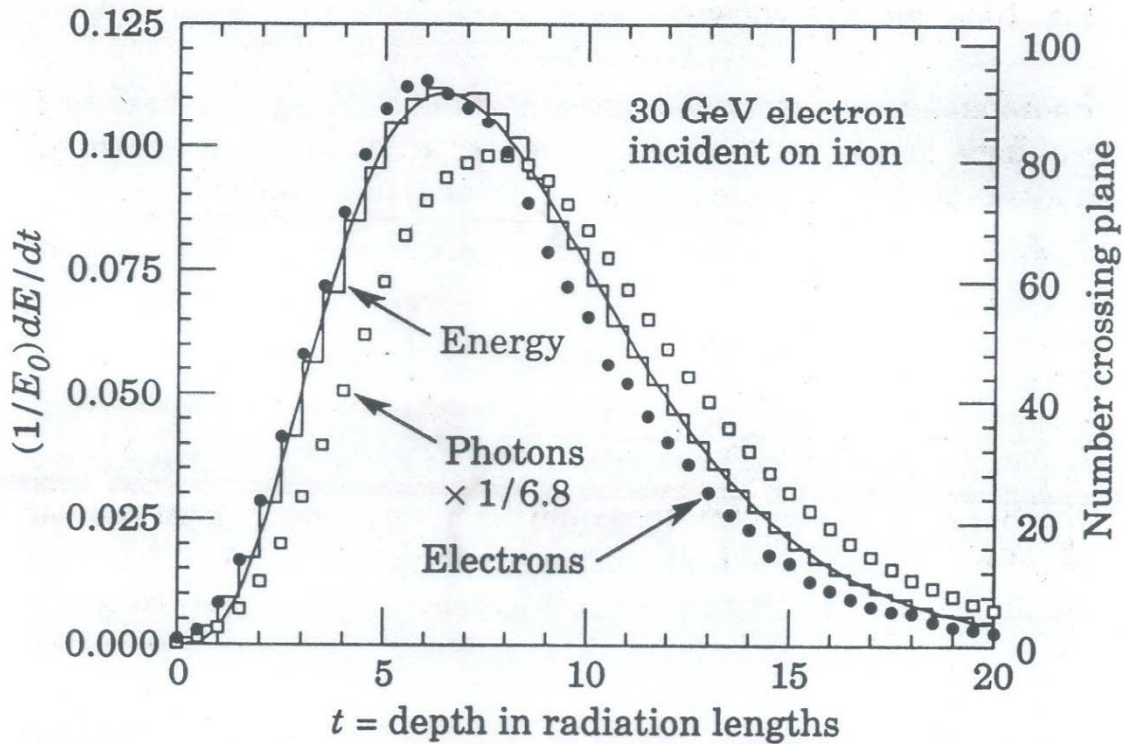
$$N = N_0 \left(\frac{x}{x_0} \right)^a e^{-b - \frac{x}{x_0}} \quad (49)$$

a, b : parametri, sibko ovisna od τ

zajetje 95% E_0

$$L \left(\frac{\Delta E}{E_0} = 95\% \right) \sim [\ln \left(\frac{E_0}{E_c} - 1 \right) + 12] X_0 \quad (50)$$

$\sim 21 X_0$ pri 100 GeV



analitični opis - Rossi '64
(Rossijeva aproksimacija B)

- $\frac{dE}{dx}$ ionizacija = $-\frac{E_c}{X_0} \neq f(E)$
- ni VCS, plaz v 1-D
- ni Comptonaovega sisanja

vz dolžni profil

$$\frac{dE}{dt} = \frac{E_0 b^{z+1}}{\Gamma(z+1)} t^z e^{-bt} \quad t = \frac{x}{X_0}$$

max. pri $t_{\max} = \frac{a}{b} = \ln \gamma_e^+ - 0,5$

$$\gamma_e^+ = \frac{E_0}{E_c}$$

skupna dolžina poti: e^\pm

$$T = \gamma X_0 = \frac{E_0}{E_c} \cdot X_0$$

\Rightarrow EM plaz odvisen je od

$$t = \frac{x}{X_0} \quad \gamma = \frac{E_0}{E_c}$$

$$\frac{1}{X_0} \sim \frac{z^2(z+1)}{A} \cdot \frac{\ln(287/\sqrt{2})}{716,4 \text{ g cm}^{-2}} \quad E_c \sim \frac{600 \text{ NeV}}{z+1,2}$$

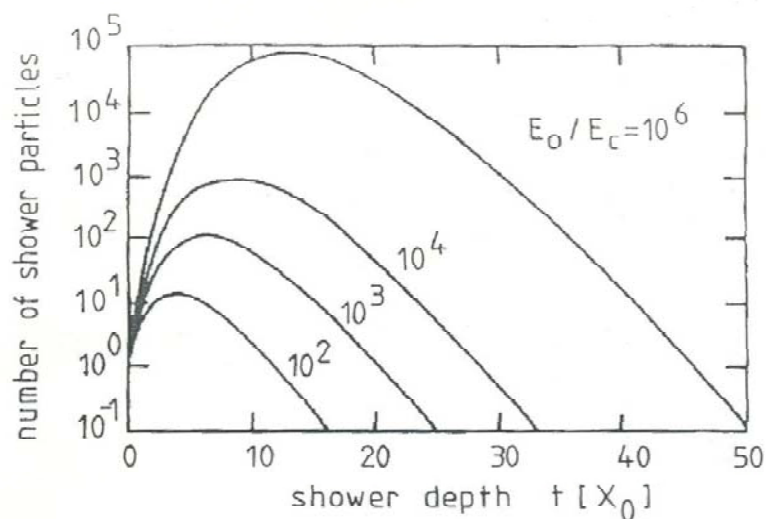


Fig. 7.21. Longitudinal shower development of electromagnetic cascades (E_c - critical energy) [509, 503].

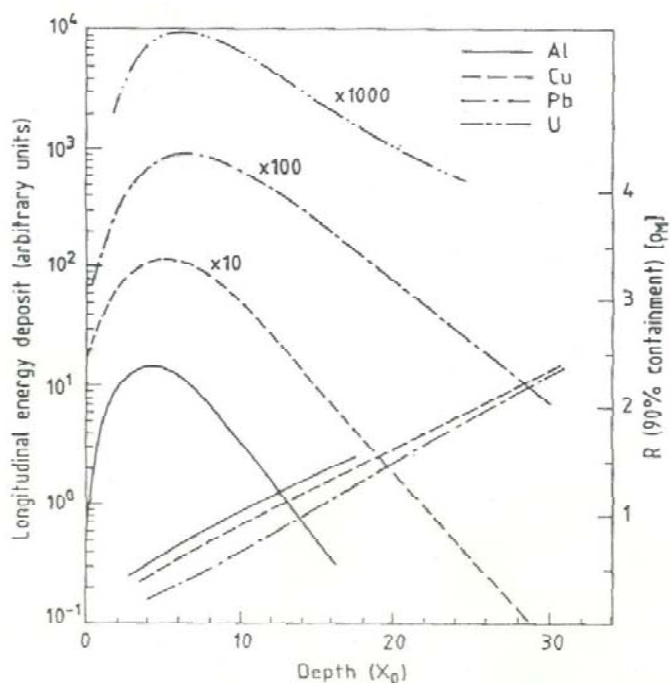


Fig. 3: Longitudinal shower development (left ordinate) of $6 \text{ GeV}/c$ electrons in four very different materials, showing the scaling in units of radiation lengths X_0 . On the right ordinate the shower radius for 90% containment of the shower is given as a function of the shower depth. In the later development of the cascade, the radial shower dimensions scale with the Molière radius $\rho_M \sim 7A/Z$. [Al, Cu, and Pb, adapted from G. Bathow et al., Nucl. Phys. B20:592 (1970). Uranium data from G. Barbiellini et al., Ref. [127].

precne dimenzije

začetek - zavorno sevanje $\propto d \left(\frac{r}{m_e}\right)^{-n_0}$
 - pari

kasneje - VCS

noliere

$$S_M = X_0 \frac{21 \text{ MeV}}{E_c}$$

različni materiali - str. 7, sl. 3., leva skala

vzdoljno širjenje plazu

1 GeV e^-

na Al

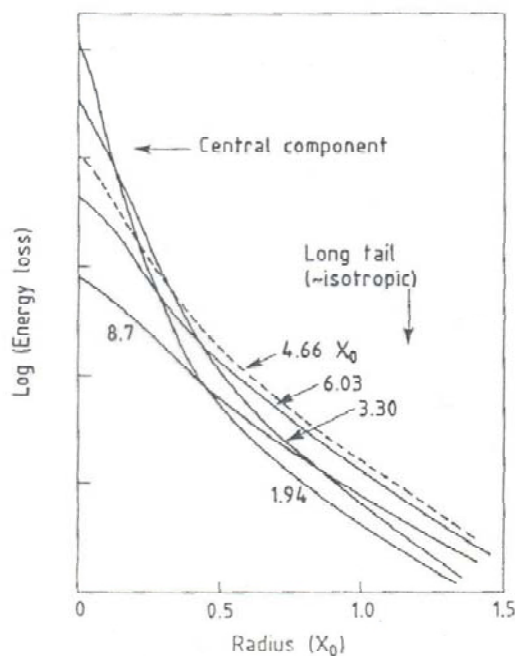


Fig. 4: Radial shower profile of 1 GeV electrons in aluminium; a pronounced central core, surrounded by 'halo', gradually widens with increasing depths of the shower [17].

c) ložljivost EM kalorimetrov

$E \rightarrow \text{plaz} \rightarrow \text{ionizacija } (T)$

→ signal: detektiramo - naboj (Si, LAr)
 (T_v) - scint. fotone (Na⁺, Cs⁺)
- Čereukove - II - (Pb steklo)

prag za detekcijo $\gamma \Rightarrow T_v < T$

$$T_v = F\left(\frac{\gamma}{E_c}\right) \frac{E}{E_c} X_0$$

$$F\left(\frac{\gamma}{E_c}\right) = \left(1 + \beta \ln \frac{\gamma}{1.53}\right) e^{\beta}$$

$$\beta = 2.29 \frac{1}{E_c}$$

ocena $N = \frac{E}{\gamma} \text{ i } \frac{T_E}{E} = \frac{1}{N}$

Pb steklo $\gamma \sim 0.7 \text{ MeV} ; \frac{T_E}{E} = \frac{45\%}{\sqrt{E[\text{Gev}]}}$

še statistika fotoelektronov

$$2,5\% \rightarrow 4\%$$

Na⁺ $E_c = 11.8 \text{ MeV} \quad \frac{1}{E_c} = 0,04$

račun

$$\left(\frac{T_E}{E}\right)_{\text{intrinsic}} = \frac{0,4\%}{\sqrt{E[\text{Gev}]}}$$

(nedoseženi) cilj graditeljev EM kalorimetrov

ločljivost je stabša od $\left(\frac{\tau_E}{E}\right)_{\text{intrinsic}}$

- statistika $\frac{\tau_E}{E} \propto \frac{1}{E}$
- puščanje
- nehomogenosti } $\tau_E \propto E$
- kalibracija
- Šum elektronike $\tau_E = \lambda_{\text{out}}$

skupaj

$$\frac{\tau_E}{E} = \frac{a}{\sqrt{E}} + b + \frac{c}{E}$$

nizke E a, c

visoke E b

druge parametri za cije

$$\frac{\tau_E}{E} \propto E^{-1/4} \quad \text{Na}, \text{Cs}$$

nehomogenosti v kristalu ($\sim a+c$)

d) vzorčevanje

homogen detektor - cena
- zbiranje signala

absorber (pasivni) Pb, W, Fe scintilator, $LAr, MWPC$
 E_c detektor

\Rightarrow vzorčevalni kalorimeter

(+) absorber: - majhen X_0 - kompakten
- poceni

detektor: - segmentiran - profil plazu
- lažje zbiranje (svetloba, el. signal)

(-) dodatne fluktuacije - slabša $\frac{\sigma_E}{E}$

Cena: štejano prehode skozi det. ravni

$$N = \frac{I}{d} \quad d - razdalja med det. rav.$$

$$N = \frac{E}{E_c} \frac{X_0}{d} = \frac{E}{\Delta E} \quad \Delta E - izguba v eni plasti$$

$$\frac{\sigma_E}{E} = \frac{1}{\sqrt{N}} = \frac{1}{\sqrt{1000}} \sqrt{\frac{\Delta E(10\text{MeV})}{E(1\text{GeV})}} = 3,2\% \sqrt{\frac{\Delta E(10\text{MeV})}{E(1\text{GeV})}}$$

$$\text{tipično: } d \sim X_0 \rightarrow \Delta E \sim E_c \sim 10\text{MeV} \Rightarrow \frac{\sigma_E}{E} \sim \frac{10\%}{\sqrt{E(\text{GeV})}}$$

ložljivost poslabša

$$- \text{VCS} : \langle d \rangle = \frac{d}{\langle \cos \theta \rangle}$$

- zaradi parov $e^+e^- N_{eff} < N$

- plinski detektor : - sisanje v ravniu : }
 - detektorija } 10x!
 - flukt uacije (Landau) } slabe!

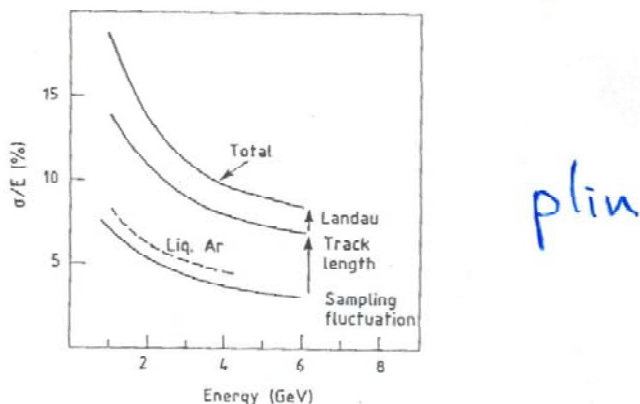


Fig. 7b: Contributions of sampling, path length, and Landau fluctuations to the energy resolution of a lead/MWPC sampling calorimeter. The latter contribute approximately equally ($\sim 12\%$ at $E = 1$ GeV), and combined quadratically with the sampling fluctuations ($\sim 7\%$) they account for the overall resolution of $\sim 18\%/\sqrt{E}$ [14].

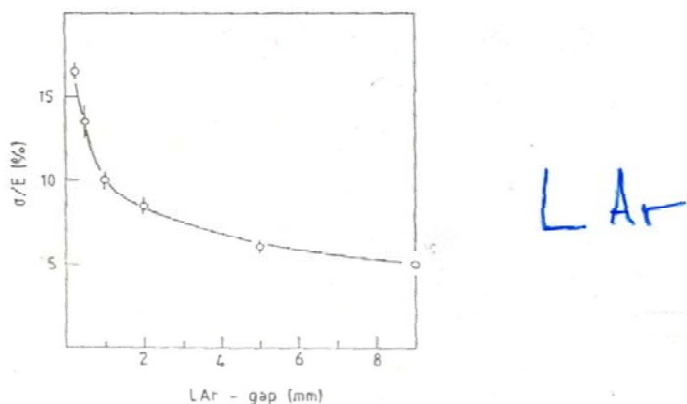


Fig. 7a: Energy resolution versus thickness of the active liquid-argon layer for 1 GeV electrons in an iron/argon sampling calorimeter.

12a

Table 28.5: Resolution of typical electromagnetic calorimeters. E is in GeV.

Technology (Experiment)	Depth	Energy resolution	Date
NaI(Tl) (Crystal Ball)	$20X_0$	$2.7\%/\sqrt{E}^{1/4}$	1983
Ba ₄ Ga ₅ O ₁₂ (BGO) (L3)	$22X_0$	$2\%/\sqrt{E} \oplus 0.7\%$	1993
CsI (KTeV)	$27X_0$	$2\%/\sqrt{E} \oplus 0.45\%$	1996
CsI(Tl) (BaBar)	$16-18X_0$	$2.3\%/\sqrt{E}^{1/4} \oplus 1.4\%$	1999
CsI(Tl) (BELLE)	$16X_0$	1.7% for $E_T > 3.5$ GeV	1998
PbWO ₄ (PWO) (CMS)	$25X_0$	$3\%/\sqrt{E} \oplus 0.5\% \oplus 0.2/E$	1997
Lead glass (OPAL)	$20.5X_0$	$5\%/\sqrt{E}$	1990
Liquid Kr (NA48)	$27X_0$	$3.2\%/\sqrt{E} \oplus 0.42\% \oplus 0.09/E$	1998
Scintillator/depleted U (ZEUS)	$20-30X_0$	$18\%/\sqrt{E}$	1988
Scintillator/Pb (CDF)	$18X_0$	$13.5\%/\sqrt{E}$	1988
Scintillator fiber/Pb spaghetti (KLOE)	$15X_0$	$5.7\%/\sqrt{E} \oplus 0.6\%$	1995
Liquid Ar/Pb (NA31)	$27X_0$	$7.5\%/\sqrt{E} \oplus 0.5\% \oplus 0.1/E$	1988
Liquid Ar/Pb (SLD)	$21X_0$	$8\%/\sqrt{E}$	1993
Liquid Ar/Pb (Hi)	$20-30X_0$	$12\%/\sqrt{E} \oplus 1\%$	1998
Liquid Ar/dept. U (D0)	$20.5X_0$	$16\%/\sqrt{E} \oplus 0.3\% \oplus 0.3/E$	1993
Liquid Ar/Pb accordion (ATLAS)	$25X_0$	$18\%/\sqrt{E} \oplus 0.4\% \oplus 0.3/E$	1996

e) hadronske plaze \rightarrow HCAL

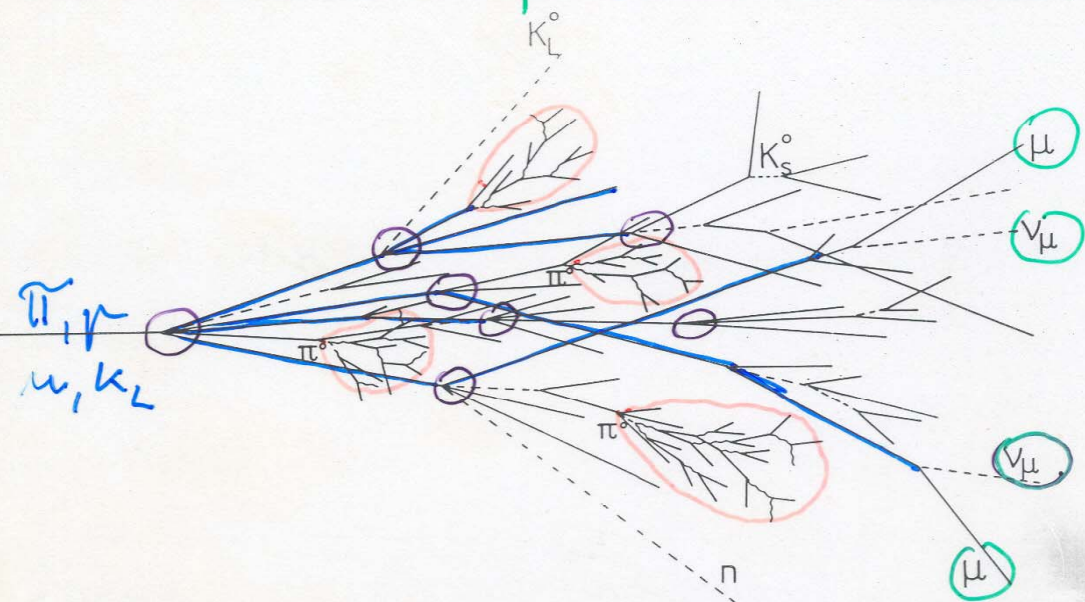


Fig. 7.32. Sketch of a hadron cascade in an absorber.

Razdelitev energije ($f(E)$, tipično za 10GeV)

- ~ 50% visokoenergijski hadroni (~ pioni) $\pi^+ \pi^-$
 \downarrow plazma
nuklearna
struktura π^0 lokalni:
 \downarrow EM plazma (X_0)
- ~ 30% počasni nukleoni $T_N < T$ signal?
- ~ 20% zvabljena jedra $\rightarrow p, n, \bar{\nu}$ 1 - ~30 MeV
- ~ $\frac{5\%}{\ln E[\text{GeV}]}$ razpad $\pi^\pm \rightarrow \mu^\pm \bar{\nu}$ pobegnejo

raznolikost procesov

\Rightarrow več možnosti za fluktacije

\rightarrow slabša ložljivost

karakteristična dolžina

$\pi^+ \pi^-$ (hadroni) interakcijska dolžina

$$\rho \lambda_I \sim 35 A^{1/3} \frac{g}{cm^2}$$

$$t = \frac{x}{\lambda_I}$$

$\pi^0 \rightarrow 2\gamma \rightarrow E\pi$ plaz X_0

$\lambda_I [cm]$ $X_0 [cm]$

Na	41	2,6
B600	23	1,1
Fe	17	1,76
Pb	18,5	0,56
U	12	0,32

\Rightarrow Fe tipičen absorber v hadronskih kalorimetrih + cena + povratni jarek magneta

maksimum plazu pri

$$t_{max} \sim 0,2 \ln(E[GeV]) + 0,7$$

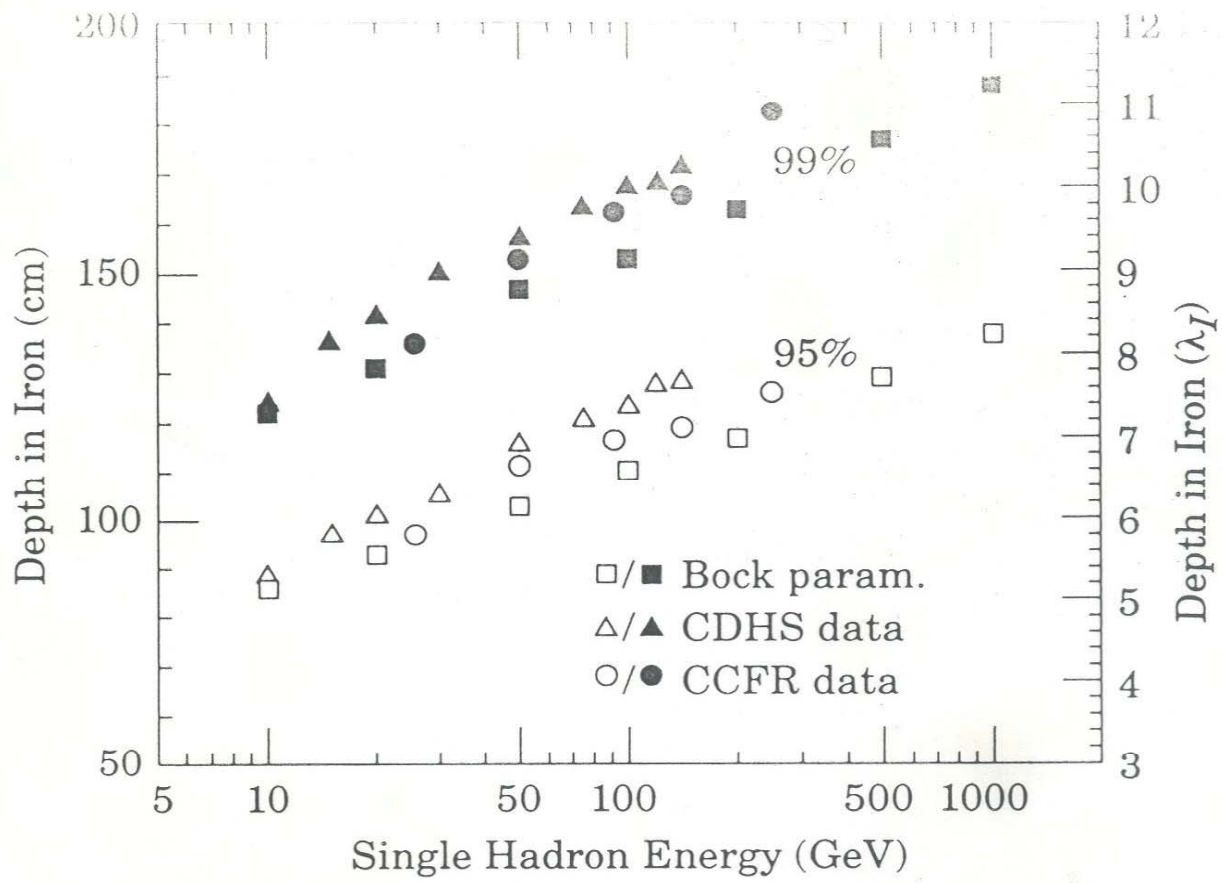


Figure 24.2: Required calorimeter thickness for 95% and 99% hadronic cascade containment in iron, on the basis of data from two large neutrino detectors and the parametrization of Bock *et al.* [44].

dolžina plazu?

a) 95% energije
v pouprečju
(ugrašankot $e^{-\frac{E}{\lambda_{att}}}$)

$$t_{95} \approx t_{\text{max}} + 2,5 \lambda_{\text{att}}$$

$$\lambda_{\text{att}} \sim (E \text{ (GeV)})^{0,13}$$

b) 95% energije
v 95% primerov

$$t_{95/95} \sim t_{95} + 3$$

fluktuacije

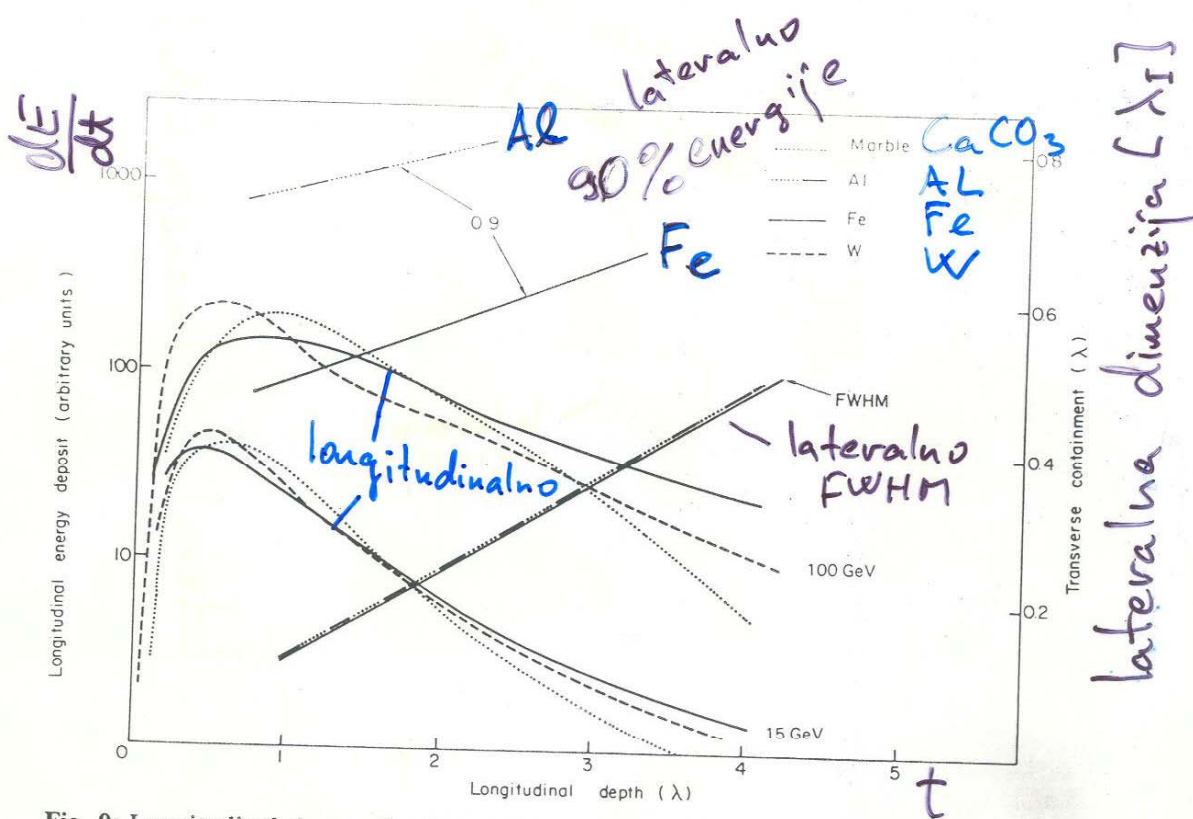


Fig. 9: Longitudinal shower development (left ordinate) induced by hadrons in different materials, showing approximate scaling in absorption length λ . The shower distributions are measured from the vertex of the shower and are therefore more peaked than those measured with respect to the face of the calorimeter. For the transverse distributions as a function of shower depth, scaling in λ is found for the narrow core (FWHM) of the showers. The radius of the cylinder for 90% lateral containment is much larger and does not scale in λ . [10 GeV/c π 's: B. Friend et al., Nucl. Instrum. Methods 136:505 (1976)]. Note that marble and aluminium have almost identical absorption and radiation lengths [Marble: M. Jonker et al., Nucl. Instrum. Methods 200:183 (1982); Fe: M. Holder et al., Nucl. Instrum. Methods 151:69 (1978); W: D.L. Cheshire et al., Nucl. Instrum. Methods 141:219 (1977)].

lateralna dimenzija

- narasča s t

- FWHM (sredica) se umeri $\propto \lambda_I$

- 90% E (rep) ni umerjen $\propto \lambda_I$

MG simulacije - opis mnogo slabši
 (GHEISHA, FLUKA) kot za EM plaz (EGS)

19

razlike med
 različnimi MC

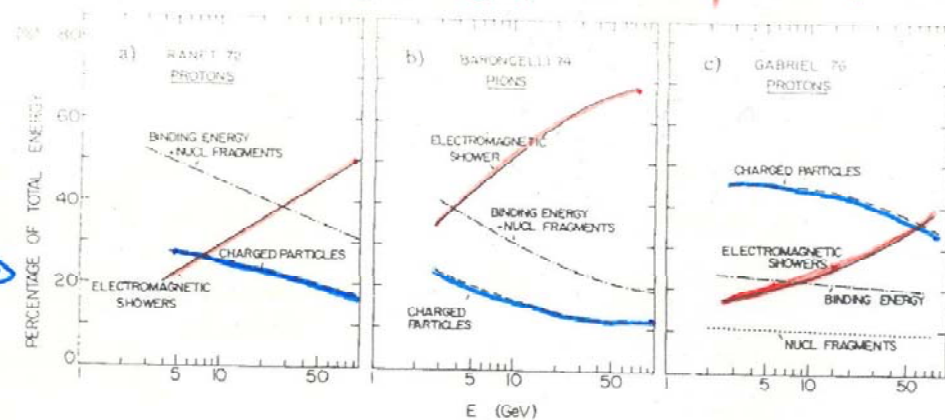


Fig. 8: Relative contributions of the most important processes to the energy dissipated by hadronic showers, as evaluated from three representative Monte Carlo calculations [25].

atmosfera

hadronski

EM

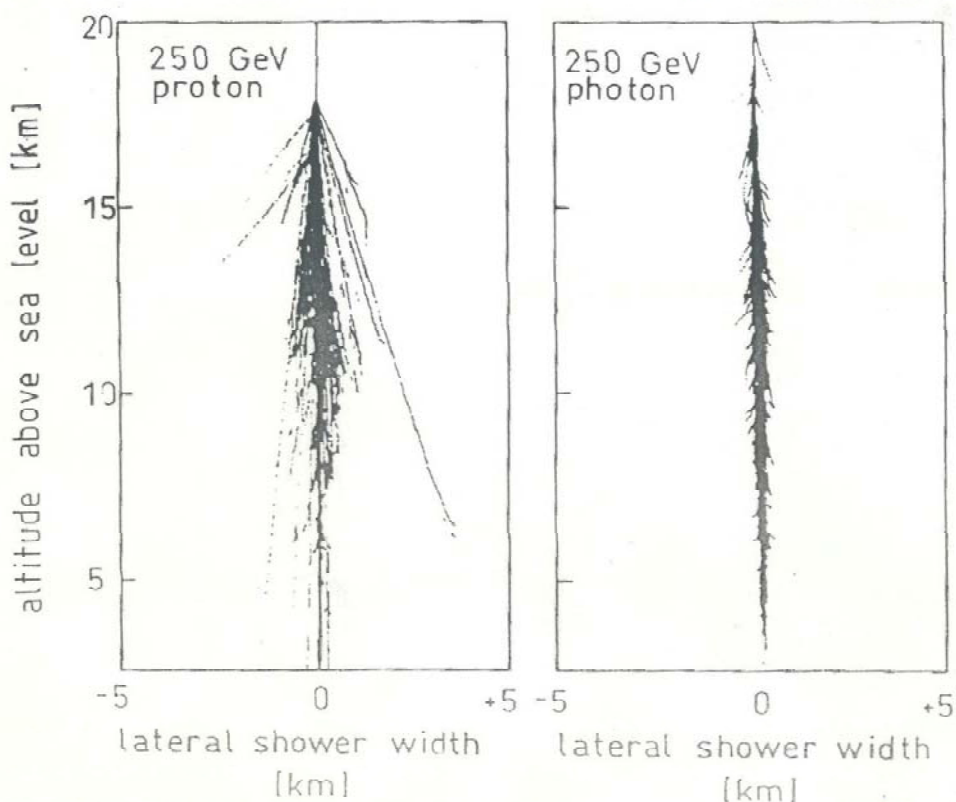


Fig. 7.34. Monte Carlo simulations of the different development of hadronic and electromagnetic cascades in the earth's atmosphere, induced by 250 GeV protons and photons [542].

f) ločljivost hadronskih Kalorimetrov 18

Omejitev

fluktuacije v razvoju plazu

- EM (π^0) ↑
- neutrini ↓
- fragmenti ↓

ločljivost mnogo slabša kot pri EM

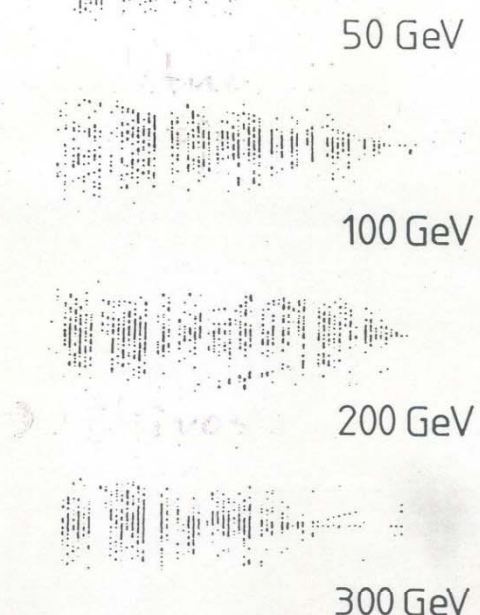
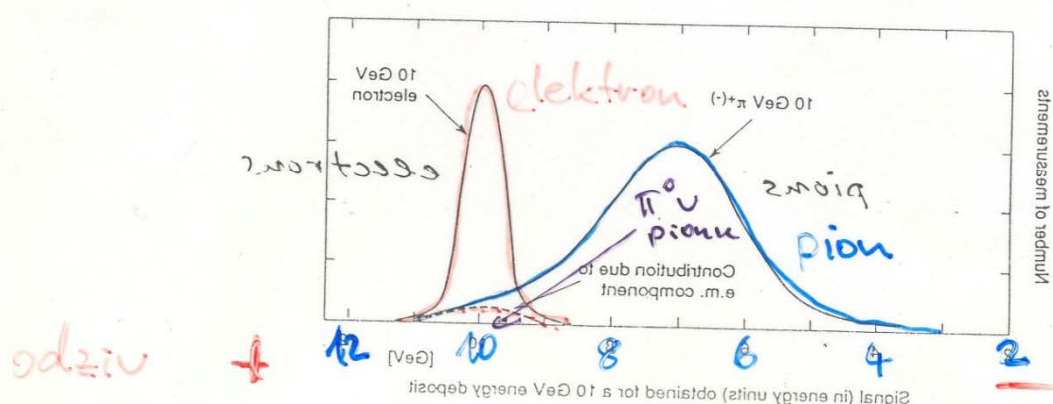


Fig. 7.42 b. Digital pattern of high energy hadron cascades (50 - 300 GeV) a flash-chamber calorimeter [560].

e/h odziv
(meritev c/π)

hadronski plaz $R_e \rightarrow \pi^0$
 $R_h \rightarrow \text{ostalo}$



$$\frac{e}{h} > 1$$

$$\Pi = e R_e + h R_h$$

\uparrow delež π^0

$$e = e \cdot 1$$

število π^0
($E > 5 \text{ GeV}$)

$$n_{\pi^0} \approx 5 \ln(E[\text{GeV}]) - 4,6$$

n_{π^0} majhuje (če pri 10 GeV) $T_{n_{\pi^0}} \sim \sqrt{n_{\pi^0}}$ velike fluktuacije R med dogodki

- $c_h \neq 1$ - $c/\pi = f(E)$ neelinearnost
- ($\sim 1,4$) - odziv nesimetričen (rep) $\Rightarrow \frac{T_E}{E} = \alpha + \frac{\beta}{E}$
- ločljivost slabša

$\frac{T_E}{E_{\text{intrinsic}}} \approx 45\%$

rešitev: kompenzacija

$$\frac{c}{\pi} \rightarrow 1$$

$$\left(\frac{T_E}{E} \right)_{\substack{c/h=1 \\ \text{intrinsic}}} \sim \frac{20\%}{\sqrt{E(\text{GeV})}} + \text{ni repov!}$$

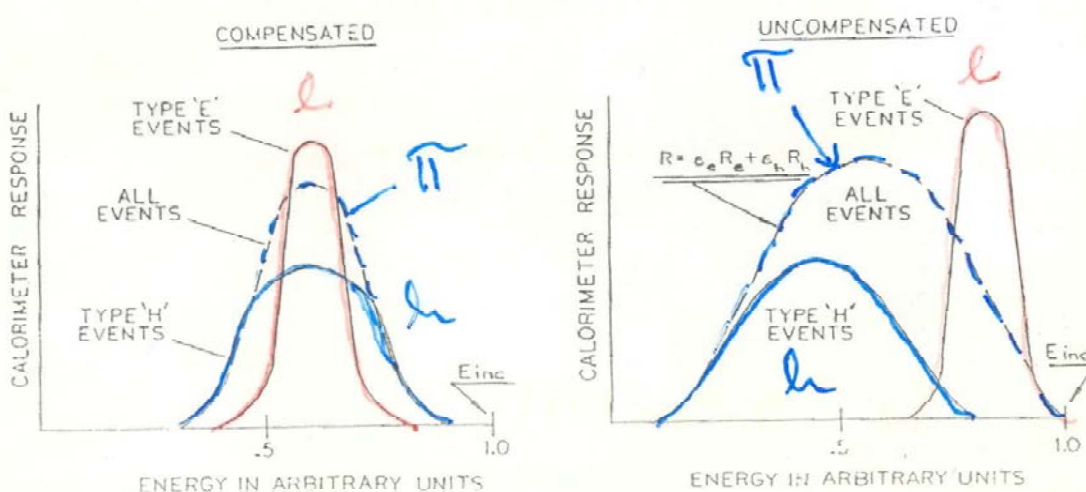


Figure 7: Schematic illustration of the effect of compensation on calorimeter response.

Kompenzacija:

- a) dvig h }
- b) zmanjšanje e } hardware
- c) meritev R_e in R_h dogodek po dogodek in uteževanje (software)

a) in b) le v vzorčevalnih kalorimetih

dvig h - detekcija neutrinoov

fisija ($\bar{\nu}$) $\rightarrow n, \gamma$
 nitek $\bar{Z} (H) \rightarrow \Delta E = E_n$

zmanjšanje e - absorber velik Z
 (fotoefekt nizkoenergijskih γ)
 $\rightarrow -40\%$ energije EM plazu
 - aktivna snov majhen Z
 (prozorna za nizkoen. γ)

$c/h \sim 1$ Pb / scintilator = 4 : 1

U / scintilator = 1 : 1

ločljivost zaradi vzorčevanja

$$\left(\frac{T_E}{E} \right)_{\text{sample}} \sim 9\% \quad \sqrt{\frac{\Delta E [\text{neV}]}{E [\text{GeV}]}}$$

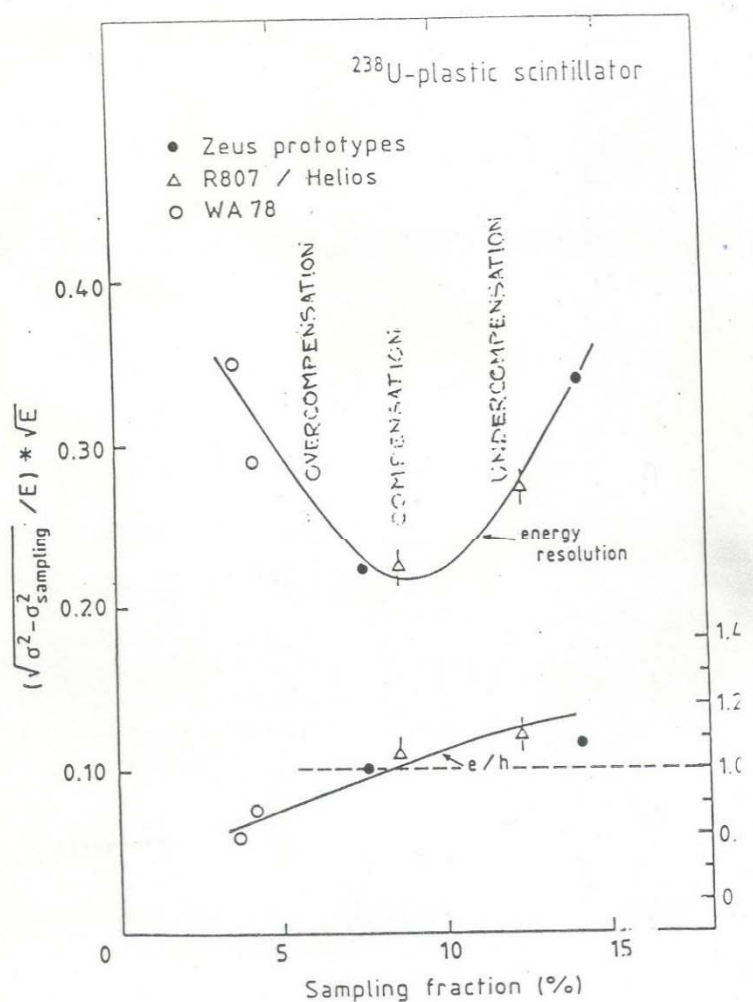
(c.f. 3,2% za EM)

$$\ll 45\% / \sqrt{E}$$

hadronski kalorimetri
vzorčevalni

Kompenzacija in variacijo razmerja 21

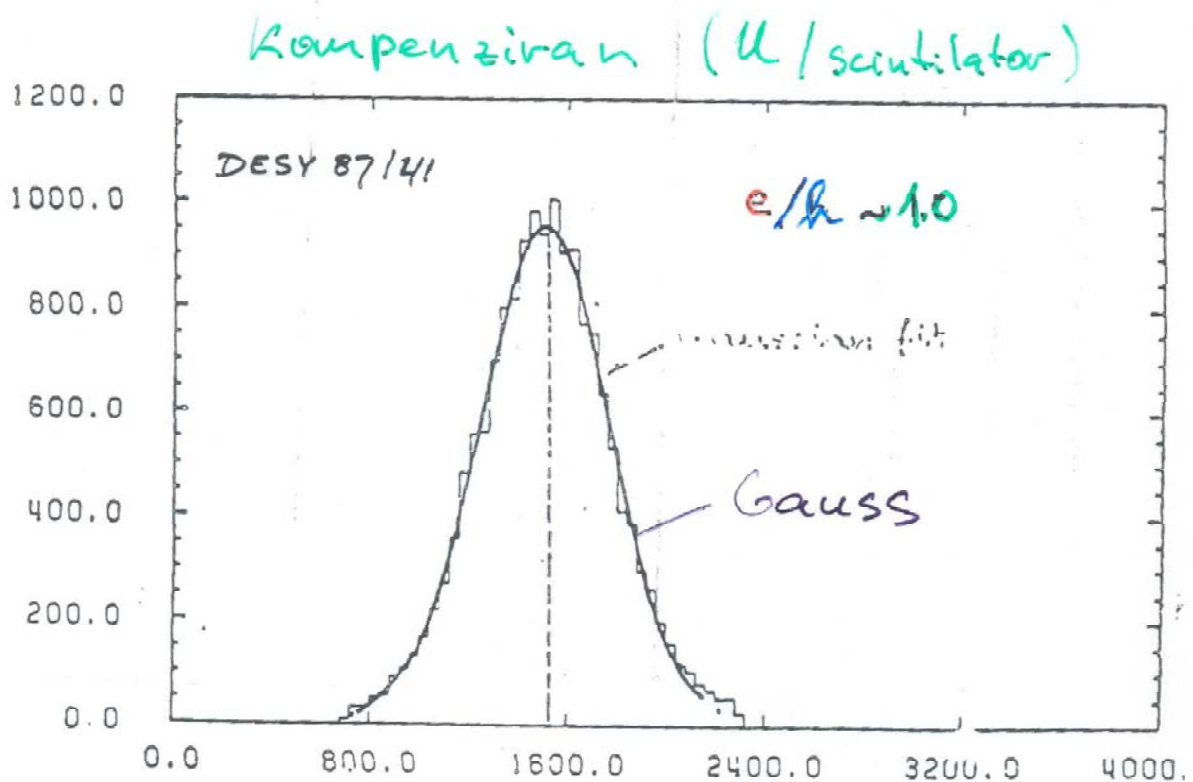
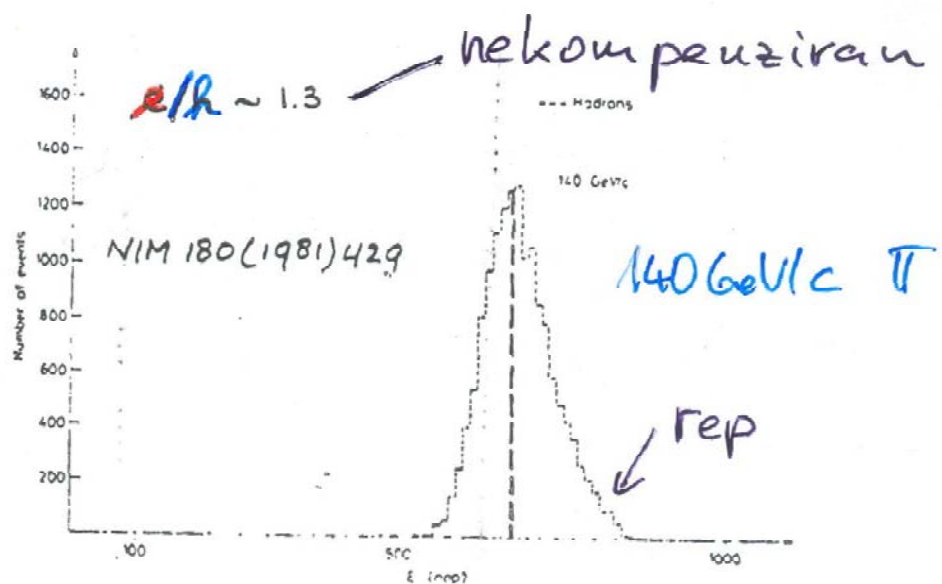
$\sigma(E)$ AND e/h AS FUNCTION OF SAMPLING FRACTION
(U-SCINTILLATOR CAL.)



optimum blizu $\frac{20\%}{\sqrt{E}}$ - teoretična meja

! možnost pre-kompenzacije ($e/h < 1$)

HADRONIC LINE SHAPE



Kompenzacija z uteževanjem
 $(R_E$ in R_L iz longitudinalnega profile plazu)

23

100 GeV π

$$\frac{R_E}{E} = \frac{80\%}{\sqrt{E}}$$

uteži

$$\frac{R_E}{E} = \frac{50\%}{\sqrt{E}}$$

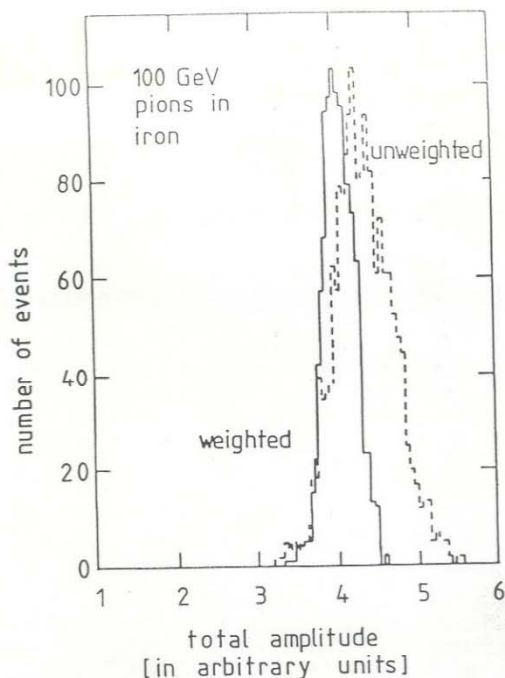


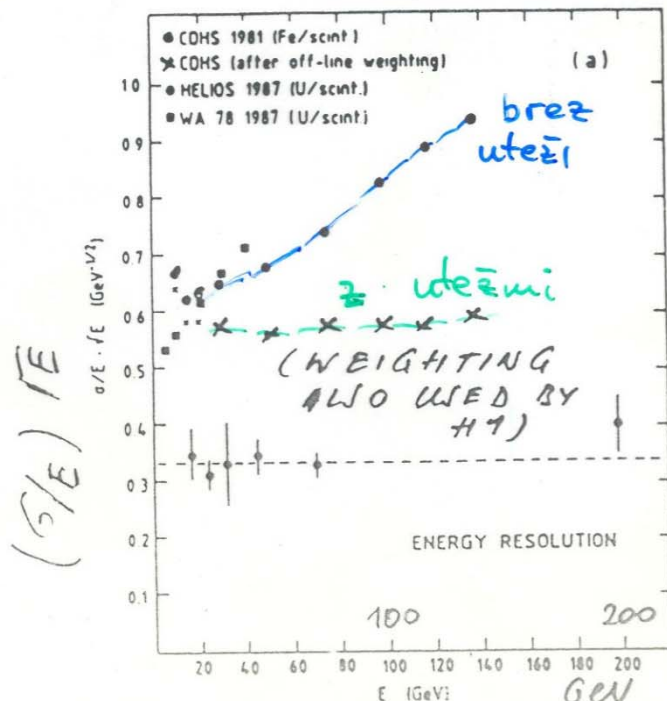
Fig. 7.45. Amplitude distribution for 100 GeV pions in an iron streamer-tube calorimeter with and without weighting factors [518]. The weighting factor was optimized for an incident energy of 100 GeV.

brez uteži

$$\frac{R_E}{E} \propto E^{-1} \quad \text{z} < 1/2$$

\pm utežmi

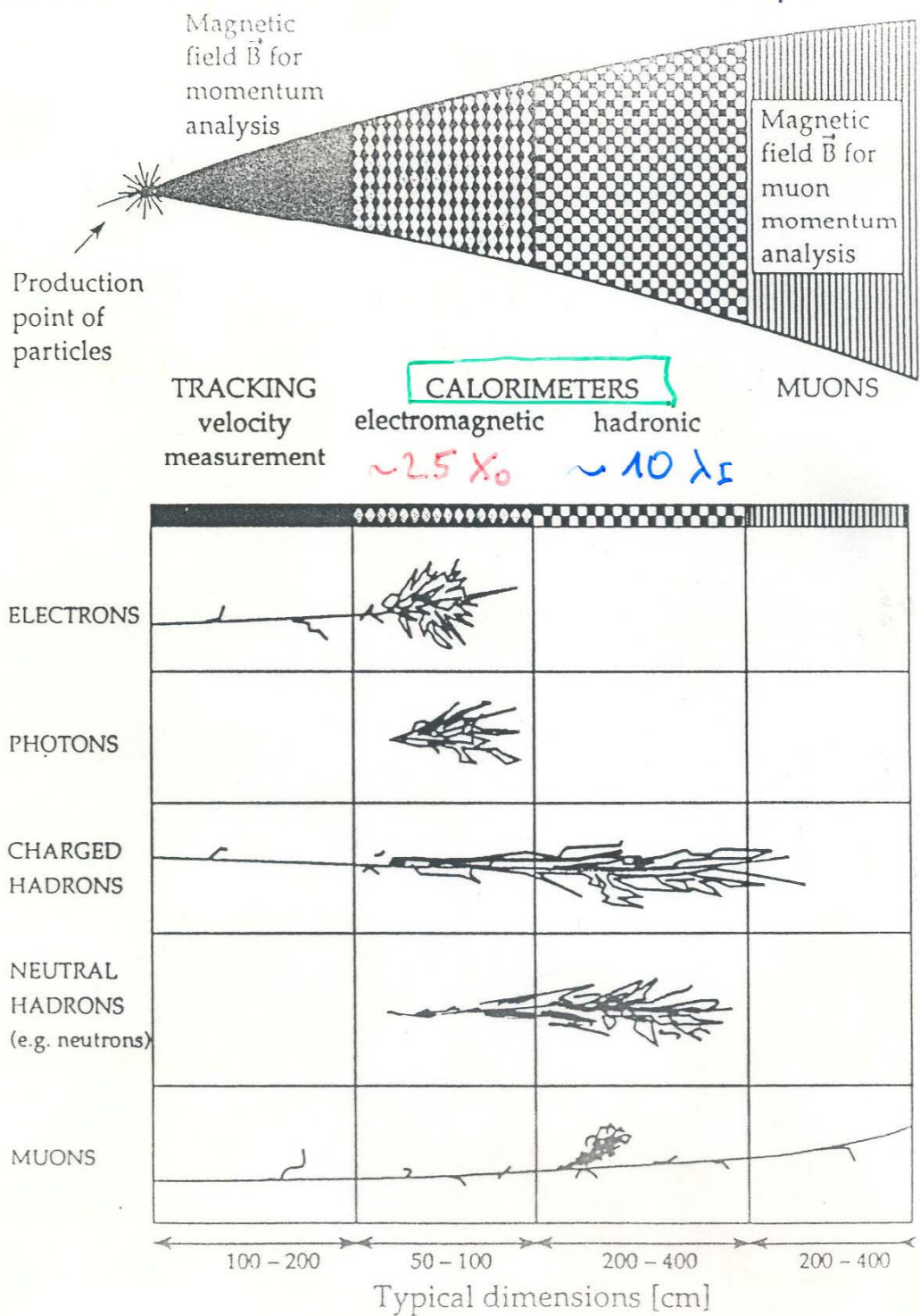
$$\frac{R_E}{E} \propto \frac{1}{\sqrt{E}}$$



g) identitika cije skalorimetri

24

Osnova: različne interakcije \rightarrow Tipunk $\mu \rightarrow$



Ivierjenje energije - osnove
kalorimetrije

26

$e \gamma \leftrightarrow \text{hadroni}$

$X_0 \leftrightarrow \lambda_I$

$$\frac{X_0}{\lambda_I} = \frac{180 A}{35 Z^2 A^{1/3}} \sim 8 Z^{-4/3}$$

0,6	neut
0,1	Fe
0,02	Per

velik Z za EM kalorimeter

\Rightarrow dobro ločevanje EM in hadronskega dela plazu

$\rightarrow e^\pm/\pi^\pm$ ločevanje (upr. za $H \rightarrow 2^{\circ} 2^{\circ} \nu_e \bar{\nu}_e$)
omejitev 1. interakcija $\pi^\pm N \rightarrow \pi^0 N$
izmenjava naboja
verjetnost $10^{-2} - 10^{-3}$

$\gamma \leftrightarrow \pi^0$ ločevanje (upr. za $H \rightarrow \gamma \gamma$)

$\pi^0 \rightarrow 2\gamma$ pod majhnim kotom

\Rightarrow zelo fino deljen prvi del ($\sim 2 X_0$)
EM kalorimetra \rightarrow pre shower

Literatura

- C. Grupen : Particle Detectors, Cambridge UP 1996
PDG : Review of Particle Physics, 1996, 2000
C. Fabjan : Calorimetry in HEP
U. Amaldi : Fluctuations in Calorimetry Measurements
v T. Ferbel : Experimental Techniques in HEP,
Addison-Wesley 1987
- H. J. Hilke : Particle Detectors, CERN Academic Training 1992
C. Fabjan : Calorimetry, ICFA '95, Ljubljana 1995